The University of Tehran Press

Pollution

Print ISSN: 2383-451X
Online ISSN: 2383-4501

https://jpoll.ut.ac.ir/

Dynamic Modeling of Urban Passenger Car Emissions in Metropolitan Tehran Based on VSP and the IVE Model

Maryam Saberiyansani | Yousef Rashidi* ✉ | Seyed Hossein Hashemi

Environmental Engineering Department, Shahid Beheshti University, Tehran, Iran

Article Info

Article type:
Research Article

Article history:
Received: 13 May 2025
Revised: 31 August 2025
Accepted: 06 February 2026

Keywords:
Traffic Dynamics
Driving Behavior
Engine Stress
Emission Modeling

ABSTRACT

Urban air pollution caused by light-duty passenger vehicles poses critical environmental and public health challenges in megacities like Tehran. In this study, we dynamically estimated vehicular emissions by collecting second-by-second speed and acceleration data from 16 representative routes, including 2 residential, 8 urban, and 6 highway segments, across metropolitan Tehran. We integrated the Vehicle Specific Power (VSP) method with the International Vehicle Emissions (IVE) model to assess real-time emission patterns across four time intervals (08:00, 12:00, 16:00, and 23:00). Our measurements showed that average speeds ranged from 14.0 to 25.97 km/h in residential areas, 10.62 to 42.13 km/h in urban corridors, and 16.43 to 67.15 km/h on highways. We found that VSP values predominantly fell within bins 8–14, reflecting acceleration-intensive and stop-and-go traffic during peak hours. We estimated emissions per kilometer as follows: CO (0.47–0.57 g), NO_x (0.11–0.23 g), CO_2 (240.7–411.5 g), VOC (0.13–0.19 g), and NMVOC (0.12–0.18 g). During peak hours, emissions increased by 40–50% compared to off-peak periods, correlating with VSP clustering around bins 8–10, while smoother traffic conditions (VSP ≥12) during off-peak hours reduced emissions. This study is among the first in the region to combine second-by-second VSP profiles with the IVE model to produce high-resolution, time-resolved urban emission estimates. Our findings highlight how dynamic traffic modeling can help policymakers design smart traffic signal systems, manage congestion, and improve air quality policies tailored to real-time conditions in megacities.

Cite this article: Saberiyansani, M., Rashidi, Y., & Hashemi, S. H. (2026). Dynamic Modeling of Urban Passenger Car Emissions in Metropolitan Tehran Based on VSP and the IVE Model. *Pollution*, 12(1), 140-152. https://doi.org/10.22059/poll.2025.395271.2934

DOI: https://doi.org/10.22059/poll.2025.395271.2934

INTRODUCTION

Air pollution is a critical environmental and public health issue in the 21st century, especially in rapidly urbanizing regions of the Global South (USEPA, 2002; Coelho et al., 2009; Wiston, 2017; Saud & Paudel, 2018). Increased industrial activity and road transport in major cities have escalated emissions of nitrogen oxides (NO_x), particulate matter (PM), carbon monoxide (CO), and non-methane volatile organic compounds (NMVOCs), contributing to local health problems and global climate change (Fernandes et al., 2021; Demetriou & Hadjistassou, 2022; Frey et al., 2022; Szopińska et al., 2022). Road transport accounts for over 40% of NO_x and 16.5% of $PM_{2.5}$ emissions in the EU, with higher shares likely in less regulated urban areas (Davison et al., 2021; Sikder et al., 2022). Light-duty vehicles are major contributors due to outdated technologies, poor maintenance, and traffic congestion (Demetriou & Hadjistassou, 2022; Saberiyansani et al., 2024).Traditional average-speed emission models fail to capture urban traffic dynamics such as acceleration and road slope (Fernandes et al., 2021; Zhong et al., 2024). The Vehicle Specific Power (VSP) method overcomes these limitations by integrating

*Corresponding Author Email: *y_rashidi@sbu.ac.ir*

speed, acceleration, slope, and resistive forces for more accurate emission estimates (USEPA, 2002; Coelho et al., 2009; Fernandes et al., 2021). However, VSP's applicability is limited where fleet composition, fuel quality, and driving behavior differ from standard assumptions (Frey et al., 2022; Saberiyansani et al., 2024).Building on VSP, the Inventory of Vehicle Emissions (IVE) model incorporates local fleet, fuel, and environmental factors, and has been successfully applied in cities including Tehran, Quito, Panama City, and New Delhi (Alipourmohajer et al., 2019; Viteri et al., 2023; Valdes-Montenegro et al., 2024; Chaudhry & Elumalai, 2024). However, IVE's use in developing megacities with high-resolution, real-time traffic data remains limited. Recent studies emphasize the importance of context-aware models reflecting regional driving patterns and fuel types, especially in low- and middle-income countries (Hao et al., 2024; Jiang et al., 2024).In Iran, while IVE has been widely used for estimating road transport emissions, its accuracy under local climatic, fleet, and traffic conditions is questioned. Studies suggest that without localized calibration and integration with field or dispersion data, IVE may not reflect real-world emissions accurately (Khazini et al., 2019; Saberiansani et al., 2024). International research advocates for enhancing traditional models with machine learning, real-time data, and hybrid approaches to improve precision (Zhang et al., 2025; Müller et al., 2025). This study aims to apply the IVE model to estimate passenger vehicle emissions in Tehran across residential, arterial, and highway roads at four daily time points (8 AM, 12 PM, 4 PM, and 11 PM). Objectives include analyzing spatial and temporal emission variations using second-by-second GPS data, evaluating IVE's accuracy under varying traffic conditions, and providing data-driven insights for urban air quality management in Tehran and similar megacities.

MATERIALS AND METHODS

This study aims to analyze driving behavior and evaluate the accuracy of the IVE model in estimating pollutant emissions from passenger vehicles in Tehran. The research process was structured into two main phases:

1. Collection of real driving behavior data using GPS technology,
2. Modeling pollutant emissions using the IVE model.

Description of the Equipment Used

To study driving behavior and calculate specific power distribution and vehicle stress based on the IVE model, it is essential to record the vehicle's driving profile and elevation changes under real conditions. The driving profile involves real-time, second-by-second speed recording, typically done using GPS devices. For this project, a GPS device connected to a battery-powered supply and capable of storing data in internal memory was used, as shown in Figure 1.

Selection of Routes for Data Collection

To accurately capture vehicle speed and elevation under real-world conditions, driving behavior was studied across diverse route types and geometries, considering factors like road incline, lane count, and urban versus highway settings. Tehran's driving conditions vary notably by region, so multiple routes were selected and categorized as follows:

• Residential Routes (2 routes): Characterized by narrow streets and lower speeds, these loop routes represent typical traffic in Tehran's residential areas.

• Urban Routes (8 routes): Covering major multi-lane streets from different geographic zones (north, south, east, west), these routes reflect varied traffic patterns in central and suburban areas during peak and off-peak hours.

• Highway Routes (6 routes): Designed to represent free-flowing traffic with higher speeds

Fig. 1. GPS device used for recording the vehicle's speed and acceleration data on a second-by-second basis

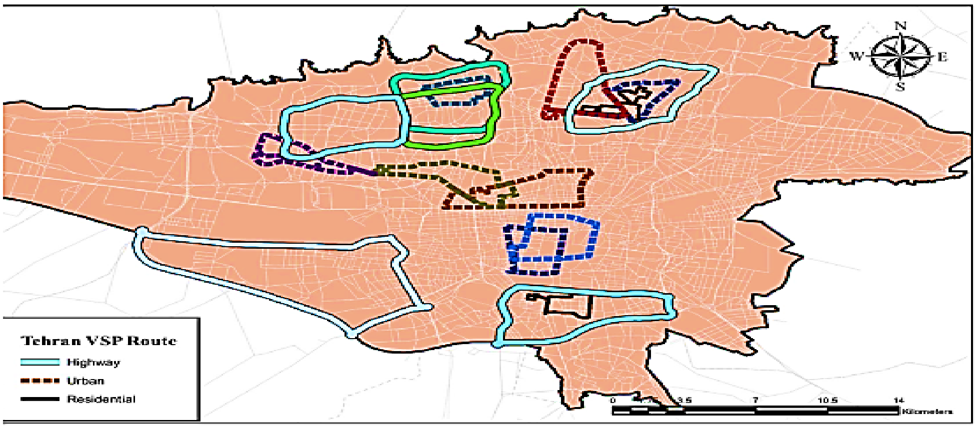

Fig. 2. Selected routes (residential, urban, and highway) on the map of Tehran

Table 1. Length of the designed routes by route type

Highway Routes		Urban Routes		Residential Routes	
Route Name	**Length (km)**	**Route Name**	**Length (km)**	**Route Name**	**Length (km)**
Highway-1	17.53	Urban-1	15.29	Residential-1	10.82
Highway-2	15.59	Urban-2	15.56	Residential-2	10.44
Highway-3	14.93	Urban-3	16.11		
Highway-4	16.63	Urban-4	15.35		
Highway-5	19.69	Urban-5	15.75		
Highway-6	31.85	Urban-6	7.83		
		Urban-7	10.78		
		Urban-8	11.24		

on at least two-lane roads, these routes capture both peak and off-peak traffic conditions.

All routes were closed loops to include a mix of positive and negative slopes. Figure 2 illustrates their locations across Tehran, spanning from south to north. Route lengths are detailed in Table 1. Data collection occurred at four time intervals (8 AM, 12 PM, 4 PM, and 11 PM) to capture diverse driving behaviors and traffic scenarios.

Calculation of Vehicle Specific Power (VSP) and Engine Stress

After collecting speed and acceleration data, the Vehicle Specific Power (VSP) for each second of driving was calculated using the following formula:

$$VSP\ (kW/ton) = v\ (m/s) * [1.1 * a\ (m/s^2) + 9.81 * \sin(\theta°) + CR] + 0.000302 * v^3\ (m^3/s^3)$$

Where:
• v: Instantaneous vehicle speed (m/s),
• a: Instantaneous acceleration (m/s^2),
• θ\theta: Road slope (degrees),
• CRCR: Rolling resistance coefficient, which was considered to be 0.013 for asphalt roads.

The coefficient 0.000302 represents the aerodynamic drag coefficient, used for standard light vehicles. This value was first introduced by Jiménez-Palacios (1999) based on aerodynamic parameters such as air density, drag coefficient, and frontal area (Jiménez-Palacios, 1999).

Additionally, the engine stress index was calculated based on the output power and engine RPM (Revolutions Per Minute) during the 5 to 25 seconds prior, using the following equation:

*Engine Stress = RPM_Index + 0.08 * PreAveragePower (kW)*

PreAveragePower = average of P(t) from t = –25 s to –5 s

The driving behavior was then classified using the distribution of VSP values into 60 bins of the IVE model (The IVE Model, n.d.).

Preparation of IVE Model Inputs

To run the IVE model, three main input files were required, as shown in Table 2:
• Fleet File: Includes vehicle type, fuel type, fueling system, usage type, and emission control and air conditioning systems.
• Location File: Contains data on local weather conditions, fuel quality (e.g., benzene, sulfur, and oxygenate levels), and local driving patterns.
• Base Adjustment File: Used to adjust coefficients and better align with real-world conditions.

RESULTS AND DISCUSSION

Driving Behavior of Passenger Vehicles

Driving behavior was analyzed using data from 16 routes (2 residential, 8 urban, 6 highway) at four time intervals (8 AM, 12 PM, 4 PM, and 11 PM). Key parameters included average and maximum speeds, along with Vehicle Specific Power (VSP) distributions from the IVE model. Detailed results are in Tables 3 and 4.

Speed Variations by Route and Time of Day

As shown in Table 3 and Figure 3, average speeds varied notably by route type and time. Highway routes consistently showed higher speeds, peaking at noon and midnight. Urban and residential routes recorded highest speeds in the morning and midnight, with residential areas showing less speed fluctuation, indicating more stable traffic. Figure 4 illustrates speed ranges, with higher speeds at midnight reflecting reduced congestion.

Comparison of Maximum Speed Across Routes

Maximum speed, depicted in Figure 5, provides further insight into route-specific driving behavior. Although no significant temporal differences are observed in urban and residential routes, the variation across different routes is more notable. This can be attributed to factors such as geometric design, road location, and traffic regulations. As anticipated, highways exhibited consistently higher maximum speeds compared to other route types across all time intervals—reinforcing the influence of route classification on driver behavior.

Distribution of Vehicle Specific Power Across Different Routes

The VSP distribution, detailed in Table 4, was analyzed for each route type and time interval.

Table 2. IVE model configuration parameters for inputs

Section	Parameter	Suggested Value / Description
Temporal and Spatial Information	Location	Tehran – By Route (Residential, Urban, Highway)
	Day of Week	X
	Altitude	Approximately 1200 meters
	A/C Use	۰ %
Fuel Characteristics	Fuel Type	Gasoline
	Sulfur Content	Low (50 ppm)
	Lead	None (Lead-free)
	Benzene	Moderate (around 1.5%)
	Oxygenate	2.5%
Vehicle Characteristics	Fleet Type	Passenger Car (Euro 4 Standard)
	I/M Class	Basic (if inspection exists) / None (if not)
	Road Grade	0.0% (Flat roads)
Driving Characteristics	Hour	Depending on conditions (e.g., 8:00 AM for peak traffic)
	Humidity	Between 30-50%
	Temperature	Between 20-30 °C
	Distance/Time	Based on collected data
	Start-ups	2 (one at start and one at end of trip)
	Fuel Mixture Characteristics	Moderate / Non-premixed (suitable for Tehran gasoline)
	Average Velocity	Calculated based on route
	VSP Bins	Determined based on speed and engine power data
Technology	Technology	Petrol, MPFI
Index	Index	Pt: Auto / Sm Tk: Med: MPFI: Euro IV: PCV / Tank: 79km
Power & Driving Variables	Power & Driving Variables	—
Fuel Quality Variables	Fuel Quality Variables	Overall Gasoline, Gasoline Sulfur, Gasoline Lead, Gasoline Benzene, Gasoline Oxygenate, Overall Diesel, Diesel Sulfur
Local Variables	Local Variables	Ambient Temperature, Ambient Humidity, Altitude Inspection
Vehicle Specific	Vehicle Specific	—
Power Road	Power Road	—
Grade Air Conditioning	Grade Air Conditioning	—
Usage Start	Usage Start	—
Distribution	Distribution	—
Maintenance Programs	Maintenance Programs	—
Base Emission Adjustment	Base Emission Adjustment	—

Although the IVE model includes 60 VSP bins, more than 95% of data points fall within bins 8–14. Therefore, the analysis focuses on this range for clarity and relevance.

Residential Routes (Figure 6): VSP distributions peak at bin 11 during noon and afternoon, indicating lower speeds and more stop-and-go movement. In contrast, higher bin shares (12–14) in the morning and midnight indicate faster, more continuous driving.

Urban Routes (Figure 7): A similar pattern to residential routes is observed, but with more distinct differences between morning and midnight. Over 50% of VSP values at midnight fall into bins 12 and above, indicating higher speed and power requirements during low-traffic periods.

Highway Routes (Figure 8): Unlike the other route types, highways show dominant shares in bin 11 during morning and afternoon, while shifting to higher bins (12–13) at noon and midnight. This suggests that even on highways, driving becomes more dynamic during low-

Table 3. Average speeds (km/h) of vehicles across different routes and time intervals

Route Name	Morning	Noon	Afternoon	Midnight
Residential-1	19.39	14.00	13.53	22.69
Residential-2	24.12	18.50	23.97	25.97
Urban-1	14.93	12.91	14.78	25.54
Urban-2	19.44	11.23	10.62	31.12
Urban-3	19.80	12.95	12.63	34.60
Urban-4	19.46	13.80	14.35	28.90
Urban-5	21.32	15.56	24.32	42.13
Urban-6	25.60	17.39	13.14	23.29
Urban-7	22.88	13.48	20.86	28.37
Urban-8	23.40	15.74	19.42	28.29
Highway-1	38.19	44.30	16.43	64.68
Highway-2	36.31	57.83	50.04	63.02
Highway-3	27.20	53.24	20.03	66.71
Highway-4	41.11	49.43	37.91	64.01
Highway-5	48.56	48.56	58.63	48.62
Highway-6	45.10	48.80	49.67	67.15

Table 4. Percentage distribution of Vehicle Specific Power (VSP) bins based on route type and time

Route	Time	Bins	Share per bin (%)
Residential	Morning	8, 9, 10, 11, 12, 13, 14, 15, 36	0.19, 1.05, 6.65, 48.66, 36.44, 6.51, 0.39, 0.08, 0.03
	Noon	7, 8, 9, 10, 11, 12, 13, 14	0.02, 0.02, 0.52, 4.84, 59.79, 30.91, 3.46, 0.44
	Afternoon	6, 7, 8, 9, 10, 11, 12, 13, 14, 15, 16, 35, 36	0.02, 0.02, 0.16, 0.97, 5.33, 56.50, 30.61, 5.19, 0.90, 0.16, 0.02, 0.05, 0.05
	Midnight	5, 6, 7, 8, 9, 10, 11, 12, 13, 14, 15, 16, 17, 18, 19, 35, 36	0.03, 0.06, 0.19, 0.62, 2.70, 8.99, 40.48, 34.29, 7.66, 2.98, 0.81, 0.50, 0.09, 0.03, 0.03, 0.03, 0.16
Urban	Morning	1, 2, 4, 5, 6, 7, 8, 9, 10, 11, 12, 13, 14, 15, 16, 17, 18, 19, 35, 36	0.01, 0.01, 0.01, 0.01, 0.06, 0.11, 0.42, 1.59, 7.40, 51.88, 27.56, 8.72, 1.78, 0.31, 0.09, 0.02, 0.01, 0.02, 0.02, 0.01
	Noon	6, 7, 8, 9, 10, 11, 12, 13, 14, 15, 16, 17, 35, 36	0.01, 0.03, 0.21, 0.88, 4.89, 66.14, 21.44, 4.82, 1.29, 0.22, 0.05, 0.01, 0.01, 0.01
	Afternoon	5, 6, 7, 8, 9, 10, 11, 12, 13, 14, 15, 16, 17, 35, 36, 37, 38	0.02, 0.01, 0.02, 0.25, 0.89, 5.10, 64.16, 21.99, 5.77, 1.40, 0.27, 0.05, 0.01, 0.01, 0.02, 0.01, 0.02
	Midnight	5, 6, 7, 8, 9, 10, 11, 12, 13, 14, 15, 16, 35, 36, 37	0.02, 0.04, 0.18, 0.55, 1.97, 6.50, 37.03, 40.83, 10.91, 1.64, 0.18, 0.02, 0.05, 0.05, 0.01
Highway	Morning	0, 1, 3, 4, 5, 6, 7, 8, 9, 10, 11, 12, 13, 14, 15, 16, 19, 35, 36, 37, 38, 39	0.03, 0.02, 0.01, 0.02, 0.03, 0.06, 0.15, 0.38, 1.17, 5.51, 35.86, 37.23, 15.17, 3.41, 0.53, 0.07, 0.02, 0.07, 0.14, 0.03, 0.03, 0.08
	Noon	0, 1, 2, 4, 5, 6, 7, 8, 9, 10, 11, 12, 13, 14, 15, 16, 17, 18, 19, 35, 36, 37, 38, 39	0.01, 0.01, 0.02, 0.06, 0.13, 0.12, 0.44, 1.13, 2.28, 7.28, 22.66, 35.58, 19.17, 8.30, 1.73, 0.12, 0.05, 0.02, 0.01, 0.62, 0.19, 0.02, 0.01, 0.05
	Afternoon	1, 3, 4, 5, 6, 7, 8, 9, 10, 11, 12, 13, 14, 15, 16, 17, 35, 36, 37, 38, 39	0.01, 0.02, 0.05, 0.04, 0.10, 0.26, 0.67, 1.58, 6.54, 44.70, 25.95, 12.43, 5.61, 1.15, 0.14, 0.01, 0.38, 0.22, 0.09, 0.05, 0.02
	Midnight	0, 1, 4, 5, 6, 7, 8, 9, 10, 11, 12, 13, 14, 15, 16, 17, 18, 29, 31, 32, 34, 35, 36, 37, 38, 39	0.02, 0.03, 0.02, 0.06, 0.15, 0.42, 0.72, 2.11, 6.40, 20.40, 28.99, 26.02, 10.96, 1.73, 0.17, 0.03, 0.02, 0.02, 0.02, 0.03, 0.81, 0.63, 0.11, 0.11, 0.30

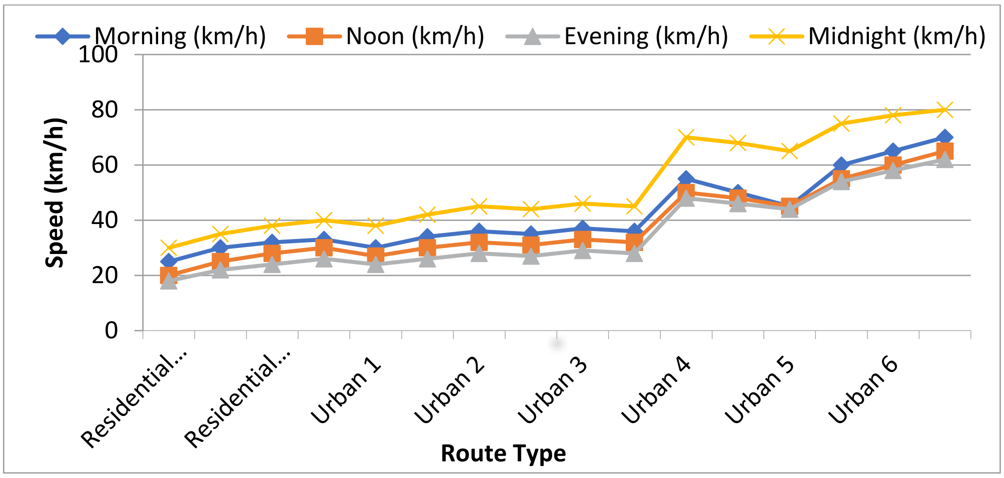

Fig. 3. Average vehicle speed across 16 sample routes at four-time intervals (8 AM, 12 PM, 4 PM, and 11 PM)

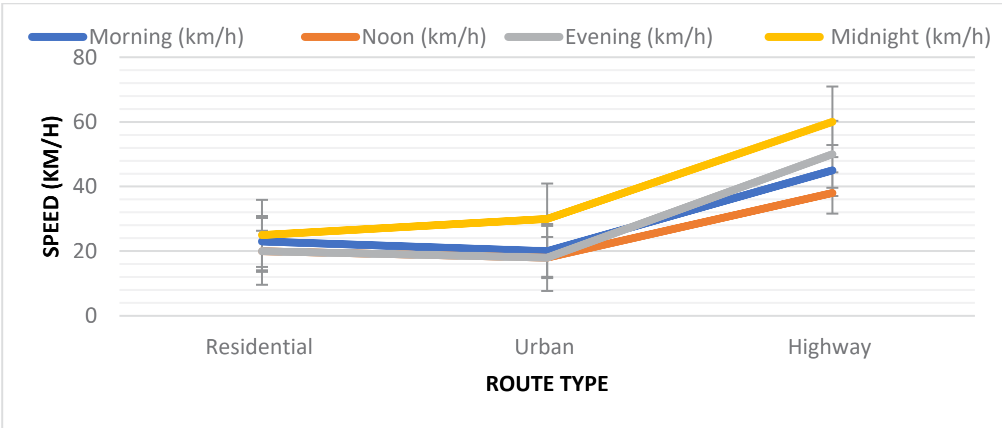

Fig. 4. Average, maximum, and minimum average vehicle speeds across three route types

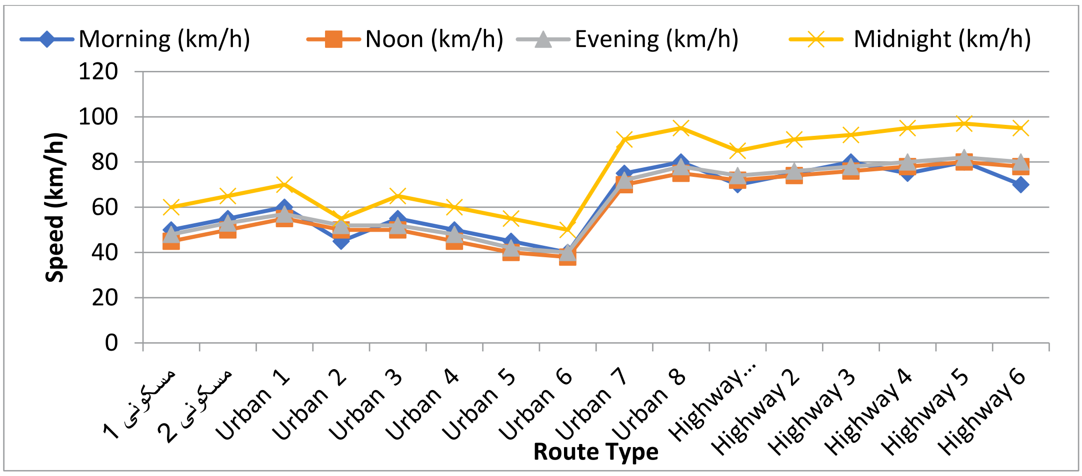

Fig. 5. Maximum recorded vehicle speeds on residential, urban, and highway routes at different times of the day

traffic periods.

An important insight from these distributions is that nearly all driving events fall within the IVE model's "low engine stress" category. For residential and urban routes, the share of high

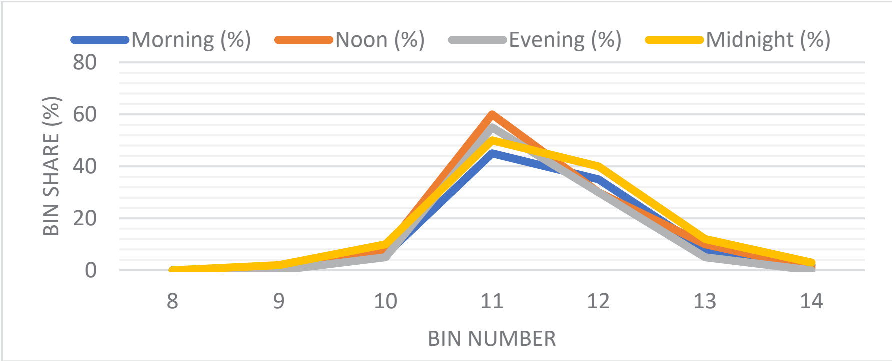

Fig. 6. Percentage distribution of VSP bins 8–14 across residential routes at four different time intervals

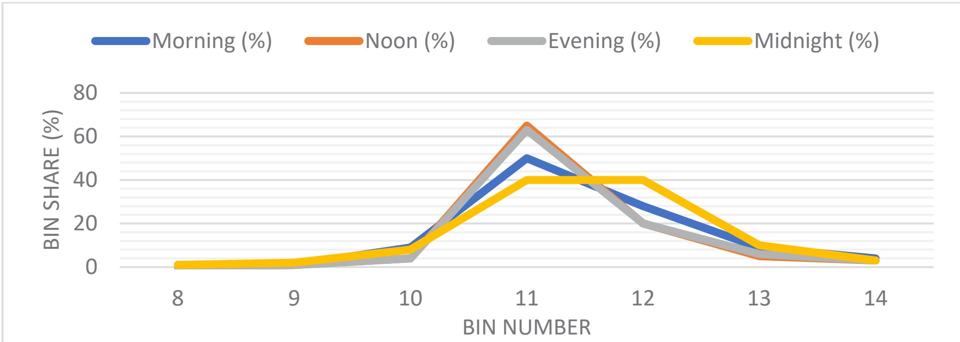

Fig. 7. Percentage distribution of VSP bins 8–14 across urban routes at four different time intervals

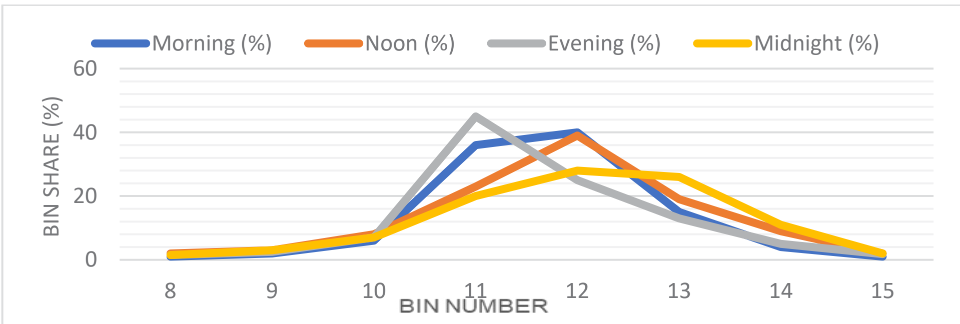

Fig. 8. Percentage distribution of VSP bins 8–14 across highway routes at four different time intervals

engine stress bins is below 0.5%, and under 2% for highway routes.

Comparison of VSP Distribution Across Route Types

Figures 9–12 present the distribution of Vehicle Specific Power (VSP) bins for urban, residential, and highway routes at different times of day:

• Morning (Figure 9): Urban routes peak at bin 11, while residential routes show significant values in bin 12. Highways display a broader spread, with over 50% of VSP values above bin 12, reflecting higher speeds and smoother flow.

• Noon (Figure 10): Bin 11 dominates urban and residential routes (>60% of VSP), whereas only 23% of highway values fall in this bin, indicating a midday shift toward higher speeds on highways.

• Evening (Figure 11): All route types cluster around bin 11, but urban and residential routes maintain relatively higher shares in upper bins, suggesting continued higher-speed driving.

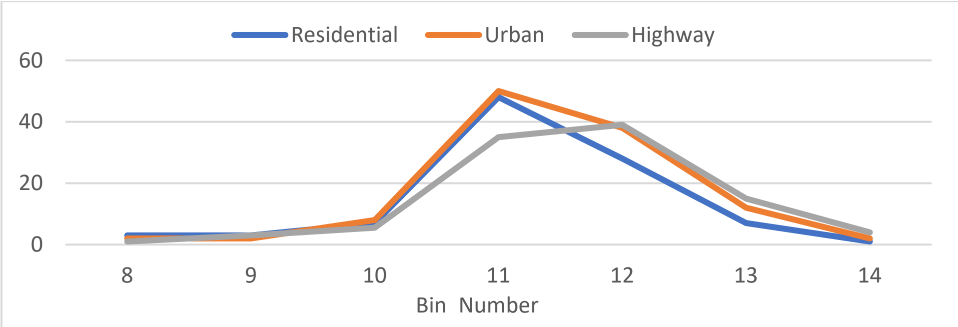

Fig. 9. Comparison of the distribution of VSP bins 8–14 across three route types in the morning

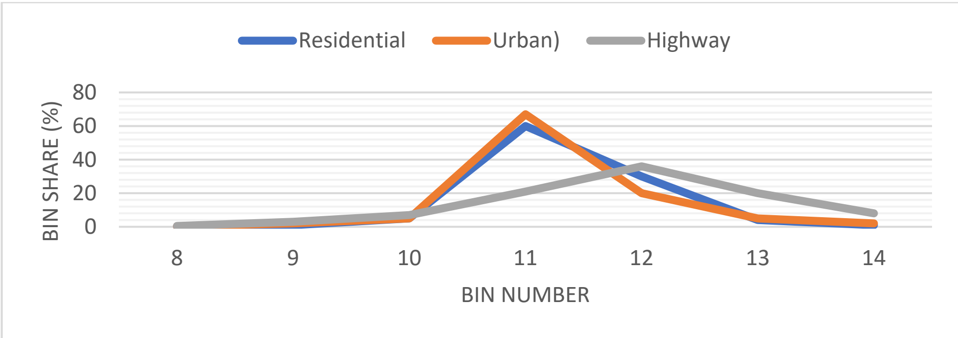

Fig. 10. Comparison of the distribution of VSP bins 8–14 across three route types at noon

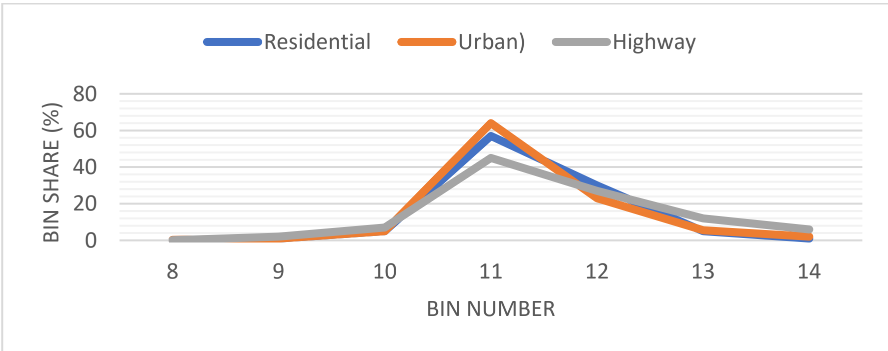

Fig. 11. Comparison of the distribution of VSP bins 8–14 among the three route types during the evening period

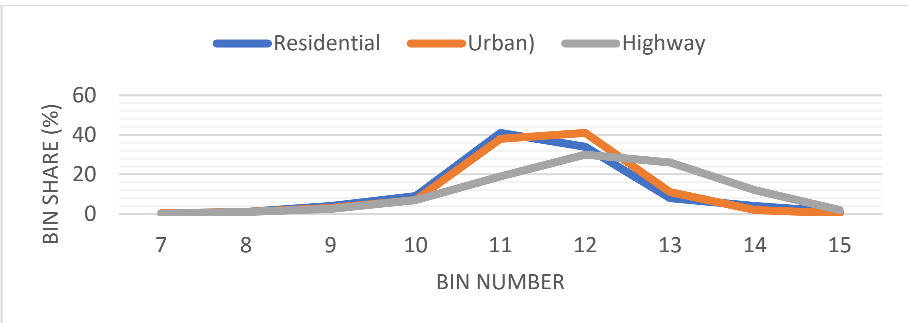

Fig. 12. Comparison of the distribution of VSP bins 8–14 among the three route types during the midnight period

Table 5. Estimated Emissions of Pollutants Based on the IVE Model

Emissions	Morning	Noon	Evening	Midnight
CO (g/km)	0.4733	0.5400	0.5700	0.5200
NOx (g/km)	0.1100	0.1400	0.2300	0.1000
CO_2 (g/km)	240.69	309.72	411.51	215.12
VOC (g/km)	0.1300	0.1600	0.1900	0.1100
NMVOC (g/km)	0.1200	0.1500	0.1800	0.1000

• Midnight (Figure 12): Urban and residential routes increase shares in bins above 12, showing smoother traffic and less congestion. Highways shift notably, with under 30% of VSP values in bins 11 or lower, indicating very high-speed, free-flow conditions.

Emission Estimates Based on the IVE Model

In this section, the emission rates of major air pollutants—including carbon monoxide (CO), nitrogen oxides (NO_x), carbon dioxide (CO_2), volatile organic compounds (VOC), and non-methane volatile organic compounds (NMVOC)—were estimated using the International Vehicle Emissions (IVE) model for four distinct time intervals: morning, noon, evening, and midnight. Emissions are expressed in grams per kilometer (g/km) and are summarized in Table 5.

Key Observations and Analysis

Diurnal Emission Patterns

Peak emissions occurred in the evening (4–6 PM) with CO_2 at 411.51 g/km and NO_x at 0.230 g/km, reflecting severe congestion, frequent stop-and-go driving, and aggressive acceleration. The lowest emissions were at midnight, with CO_2 at 215.12 g/km and NO_x at 0.100 g/km, corresponding to lower traffic and smoother driving.

Pollutant Interactions

The CO_2-to-NO_x ratio dropped from about 2197 in the morning to 1790 in the evening, indicating a disproportionate rise in NO_x during congestion. VOC and NMVOC emissions followed the NO_x pattern, peaking in the evening and falling at midnight, linked to engine load and driving aggressiveness.

Impact of Vehicle Specific Power (VSP)

Evening dominance of VSP bins 10–12 suggests higher engine loads and acceleration, increasing fuel consumption and emissions. Midnight distributions shifted to more efficient bins (6–9), consistent with steady speeds and less idling, explaining lower emissions.

Implications for Traffic and Air Quality Management

Smoothing traffic flow—reducing stops, idle times, and promoting steady speeds during rush hours—could substantially cut NO_x and CO_2 emissions. Strategies like adaptive traffic signals, congestion pricing, and better public transit at peak times are recommended. The IVE model offers valuable time-resolved emission insights for dynamic air quality policies over static average-based approaches.

CONCLUSION

This study applied second-by-second GPS speed and acceleration data from 16 routes in

Tehran—covering residential, urban, and highway corridors—to estimate real-world emissions using the IVE model. Results showed strong temporal and spatial emission variations linked to VSP distributions. The IVE model effectively captured CO_2, NO_x, and CO emissions in Tehran's complex traffic environment, aligning with successful applications in cities like Quito and Panama City (Viteri et al., 2023; Valdes-Montenegro et al., 2024). Peak traffic periods featured over 60% of operations in high VSP bins (10–12), associated with congestion and high emissions ($CO_2 \geq 410$ g/km, $NO_x \geq 0.23$ g/km). Off-peak periods, especially midnight, showed smoother flows and lower emissions.Highways consistently recorded the highest speeds (up to 67 km/h at midnight), while residential routes had more stable traffic, supporting prior findings on emissions benefits of steady driving (Coelho et al., 2009).

Limitations and Future Directions

The study is limited by its focus on 16 routes during a single season and lacks meteorological and dispersion modeling, crucial for understanding pollutant fate. Future work should expand spatial-temporal coverage, integrate atmospheric flow models (e.g., WRF-Chem, CALPUFF), include more pollutants ($PM_{2.5}$, O_3), and combine IVE outputs with real-time monitoring. Incorporating machine learning or hybrid models could further improve prediction accuracy.

Comparison with Previous Work

Building on our prior study comparing COPERT and IVE models (Saberiyansani et al., 2025), this research highlights the importance of second-by-second driving variability and VSP dynamics, providing a more realistic emission profile than average-speed methods.

Final Remark

Integrating high-resolution driving behavior with the IVE model offers a robust, transferable framework for dynamic emission estimation. To advance beyond data reporting, future studies should combine atmospheric science, meteorology, and advanced data fusion. These findings form a solid basis for developing targeted emission control strategies and sustainable urban transport policies in Tehran and similar megacities.

Declarations

- Funding: No financial support was received.
- Conflicts of Interest: None declared.
- Ethical Approval: No biological or life science experiments were conducted.

ACKNOWLEDGEMENTS

The authors would like to express their sincere appreciation to the *Tehran Air Quality Control Company (AQCC)* for providing access to emission-related data and technical consultation. Their support played a critical role in the successful execution of this research.

GRANT SUPPORT DETAILS

The present research did not receive any financial support.

CONFLICT OF INTEREST

The authors declare that there is not any conflict of interests regarding the publication of this manuscript. In addition, the ethical issues, including plagiarism, informed consent, misconduct, data fabrication and/or falsification, double publication and/or submission, and redundancy have been completely observed by the authors.

LIFE SCIENCE REPORTING

No life science threat was practiced in this research.

REFERENCES

Alipourmohajer, S., Rashidi, Y. and Atabi, F. (2019). Verification of IVE Model for SAIPA Co. Fleet Emission. Pollution, 5(2); 235-245.

Atuyambe, L.M., Arku, R.E., Naidoo, N., Kapwata, T., Asante, K.P., Cissé, G., Simane, B., Wright, C.Y. and Berhane, K. (2024). The health impacts of air pollution in the context of changing climate in Africa: A narrative review with recommendations for action. Ann. Glob. Health, 90(1); 76.

Avenue in Panama City, Panama. (2024). E3S Web of Conferences (ICFEE 2024).

Azevedo, J.A.H., Cassiano, D.R. and Bertoncini, B.V. (2024). Real driving cycles and emissions for urban freight transport. Front. Big Data, 7; 1375455.

Chaudhry, S.K. and Elumalai, S.P. (2024). Assessment of sustainable school transport policies on vehicular emissions using the IVE model. J. Clean. Prod., 434; 140437.

Coelho, M.C., Frey, H.C., Rouphail, N.M., Zhai, H. and Pelkmans, L. (2009). Assessing methods for comparing emissions from gasoline and diesel light-duty vehicles based on instantaneous emissions data. Sci. Total Environ., 408(2); 336–345.

Coelho, M.C., Frey, H.C., Rouphail, N.M., Zhai, H. and Pelkmans, L. (2009). Assessing methods for comparing emissions from gasoline and diesel light-duty vehicles based on microscale measurements. Transp. Res. Part D, 14(2); 91–99.

Davison, J., Rose, R.A., Farren, N.J., Wagner, R.L., Murrells, T.P. and Carslaw, D.C. (2021). Verification of a national emission inventory and influence of on-road vehicle manufacturer-level emissions. Environ. Sci. Technol., 55(8); 4452–4461.

Demetriou, E. and Hadjistassou, C. (2022). Lowering mortality risks in urban areas by containing atmospheric pollution. Environ. Res., 211; 113096.

Development and Application of IVE (Part 3: Developing Countries Team) (2024). E3S Web of Conferences.

Fernandes, P., Bandeira, J., Silva, C.M. and Coelho, M.C. (2021). Comparison of models to predict NO_x and CO_2 emissions based on real-world driving parameters. Sci. Total Environ., 765; 144391.

Frey, H.C. et al. (2022). Characterizing determinants of near-road ambient air quality for an urban intersection and a freeway site. Health Effects Inst. Res. Rep., 207; 1–73.

Ghaffarpasand, O., Alipourmohajer, M. and Rashidi, Y. (2021). Evaluation of VSP-based driving behavior on emission estimates using the IVE model.

Hao, J., Yang, Z., Zhang, R., Ma, Z., Liu, J., Bi, H. and Guo, D. (2024). Crosstalk between heredity and environment in myopia: An overview. Heliyon, 10(8); e29715.

Jiang, Z., Wu, L., Niu, H., Jia, Z., Qi, Z., Liu, Y., Zhang, Q., Wang, T., Peng, J. and Mao, H. (2024). Investigating the impact of high-altitude on vehicle carbon emissions: A comprehensive on-road driving study. Sci. Total Environ., 918; 170671.

Jiménez-Palacios, L. (1999). Vehicle specific power: A useful parameter for remote sensing and emission studies. 9th CRC On-Road Vehicle Emissions Workshop, San Diego, USA.

Khazini, L., Jamshidi Kaljahi, M. and Blond, N. (2019). Investigation of emission levels and dispersion patterns of pollutants from vehicles in Tabriz city. Civ. Environ. Eng. J., 49(96); 23–34.

Liu, H., Guensler, R., Lu, H., Xu, Y., Xu, X. and Rodgers, M.O. (2019). MOVES-Matrix for high-performance on-road energy and running emission rate modeling applications. J. Air Waste Manag. Assoc., 69(12); 1415–1428.

Müller, T., Schneider, A. and Braun, M. (2025). Integration of real-time floating car data with COPERT 5.6 for dynamic urban emission modeling in Germany. Environ. Sci. Technol., 59(2); 1456–1472.

Saberiyansani, M., Rashidi, Y. and Hashemi, S.H. (2024). Comparison of the real emissions of domestic passenger cars with the IVE model. Environ. Sci., 22(1); 39–52.

Saberiyansani, M., Rashidi, Y. and Hashemi, S.H. (2025). Comparative analysis of COPERT and IVE models in road transport emission assessment. Sustain. Earth Trends, 5(3); 25–35.

Saud, B. and Paudel, G. (2018). The threat of ambient air pollution in Kathmandu, Nepal. J. Environ. Public Health, 2018; 1504591.

Sikder, M., Wang, C., Yao, X., Huai, X., Wu, L., KwameYeboah, F., Wood, J., Zhao, Y. and Dou, X. (2022). The integrated impact of GDP growth, industrialization, energy use, and urbanization on CO_2 emissions in developing countries: Evidence from the panel ARDL approach. Sci. Total Environ., 837; 155795.

Singh, A., Sharma, P. and Kaur, G. (2023). Assessment of vehicular emissions in New Delhi using real-world VSP-based analysis. Transp. Res. Part D, 115; 103565.

Szopińska, K. et al. (2022). Verification of the perception of the local community concerning air quality using ADMS-Roads modeling. Int. J. Environ. Res. Public Health, 19(17); 10908.

The IVE Model. (n.d.). International Vehicle Emissions Model.

United States Environmental Protection Agency (USEPA). (2002). Comprehensive Modal Emission Model (CMEM) User's Guide (EPA420-R-02-007). Office of Transportation and Air Quality.

Valdes-Montenegro, A., Gonzalez-Olivardia, F., Thepanondh, S. and Pinzón-Acosta, C. (2024). Estimation of on-road mobile emissions based on the vehicle technology in a high-traffic avenue in Panama City, Panama. E3S Web Conf., 530; 01003.

Valdes-Montenegro, D., Gómez, R. and Ortega, M. (2024). Adapting the IVE model for emission estimates in Panama City. Urban Clim., 49; 101770.

Viteri, M., Guevara, M. and Espinosa, L. (2023). Evaluation of truck-related CO hotspots using the IVE model in Quito, Ecuador. Environ. Monit. Assess., 195(3); 243.

Viteri, R., Borge, R., Paredes, M. and Pérez, M.A. (2023). A high-resolution vehicular emissions inventory for Ecuador using the IVE modelling system. Chemosphere, 315; 137634.

Wiston, M. (2017). Status of air pollution in Botswana and significance to air quality and human health. J. Health Pollut., 7(15); 8–17.

Zhang, L., Huang, Y. and Wu, Q. (2025). Spatiotemporal vehicle emission prediction in megacities using hybrid IVE-LSTM models: A case study of Shanghai. Atmos. Environ., 312; 119921.

Zhong, H., Chen, K., Liu, C., Zhu, M. and Ke, R. (2024). Models for predicting vehicle emissions: A comprehensive review. Sci. Total Environ., 923; 171324.

Zhou, Y., Li, H. and Zhang, Y. (2022). Dynamic emission modeling based on driving patterns in Shanghai. J. Environ. Sci., 112; 245–253.